Time-Dependent Signatures of Acoustic Wave Biosensors

WILLIAM D. HUNT, DESMOND D. STUBBS, AND SANG-HUN LEE

Invited Paper

Acoustic wave devices coated with a biolayer represent one biosensor approach for the detection of medically relevant biomolecules. In a typical application, the acoustic wave device is connected in an oscillator circuit, and the frequency shift Δf resulting from a biomolecular event is recorded. In this paper, we discuss our recent work in this field, which has included the use of Rayleigh wave surface acoustic wave devices for vapor phase detection as well as quartz crystal microbalance devices for liquid phase measurements. For all of the results reported herein the biofilm on the surface of the acoustic wave device consists of a layer of antibodies raised against a specific target molecule or antigen. We present our results for the vapor phase detection of small molecules such as uranine and cocaine as well as liquid phase detection of small and large molecules. The data we present from these various experiments is the signature associated with the biomolecular recognition events; that is, we record and present $\Delta f(t)$. Finally, we present the recent results of our time-dependent perturbation theory work, which gives a potential method for resolving the acoustic wave biosensor signature into information relating to molecular structure changes during a molecular recognition event.

Keywords—Acoustic sensors, biosensors, bulk acoustic wave (BAW), quartz crystal microbalance (QCM), surface acoustic wave (SAW).

I. BACKGROUND AND INTRODUCTION

Acoustic sensors represent an approach for high-precision sensing that has been highly successful and has had a long history of reduction to practice. Quartz crystal microbalances

Manuscript received February 2, 2003; revised March 20, 2003.

W. D. Hunt is with the School of Electrical and Computer Engineering, Georgia Institute of Technology, Atlanta, GA 30332 USA (e-mail: Bill.Hunt@ee.gatech.edu). He is also with the Department of Hematology and Oncology, Emory University School of Medicine, Atlanta, GA 30332 USA.

D. D. Stubbs is with the School of Chemistry and Biochemistry, Georgia Institute of Technology, Atlanta, GA 30332 USA (e-mail: Desmond.Stubbs@chemistry.gatech.edu).

S.-H. Lee is with the School of Electrical and Computer Engineering, Georgia Institute of Technology, Atlanta, GA 30332 USA (e-mail: gt6361b@prism.gatech.edu.)

Digital Object Identifier 10.1109/JPROC.2003.813566

(QCMs) were there at the dawn of the semiconductor industry, having been utilized since the 1950s [1] to monitor the thickness of metals being deposited on wafers in evaporation systems. From the start, this was a sensor technology which leveraged investments in other technologies, namely, oscillator designs and electronic frequency counters. In addition, the investments in frequency control and radar during World War II and for the quarter century that followed led to a detailed understanding of the temperature characteristics of quartz, largely at the Ft. Monmouth, NJ, Army Research Lab in the United States. In cuts of quartz such as the AT-cut used for QCM, the linear expansion of the material with increasing temperature is compensated by an increase in the acoustic velocity such that the round trip delay for an acoustic wave in a resonator does not vary with temperature. Further, from an instrumentation standpoint, it has been argued that acoustic wave sensors in this oscillator configuration represent a highly advantageous approach to sensing precisely because slight shifts (ppb) in frequency are far easier to measure than equivalent perturbations in a voltage or current.

This paper deals with acoustic wave biosensors, and it is reasonable to begin with a description or definition of what we mean by "biosensor." In general, biosensors are distinguished from chemical sensors in that they use a molecule of biological origin (e.g., antibody, cell, enzyme) immobilized onto a surface as the chemically sensitive film on a device [2]. The colloquial view of the term is that "biosensors" refers to devices which detect the presence of entities of biological origin, such as proteins or cells, and that this detection *must* take place in a liquid. We have demonstrated recently that an acoustic sensor with an immobilized biofilm need not be restricted to the detection of biomolecules, and the detection environment need not be limited to the liquid phase [3]–[5].

In this paper, we will discuss our acoustic wave biosensors which utilize biomolecules, specifically IgG monoclonal antibodies, to achieve molecular recognition in the vapor phase and liquid phase as well. For immunoassay techniques such as this, antibodies, specific for a target antigen, are utilized

as the chemically specific receptor molecule. The production of these monoclonal antibodies by the hybridoma technique was first reported by Kohler and Milstein [6]. This technique made it possible to produce antibodies in large quantities using cultures of myeloma cells fused with lymphocytes raised against the target antigen. A culture of the resulting hybrid cells (a.k.a. hybridoma cells) synthesizes the antibody of the parent lymphocyte and has the immortality of the myeloma cancer cell with which the lymphocyte was fused. Antibodies have been generated for a wide variety of antigens and are commercially available from numerous industrial sources such as Sigma-Aldrich and Accurate Chemical, among others.

We collect the time course of the frequency shift before, during, and after a binding event which forms a signature in the form of $\Delta f(t)$ for each of the biomolecular events we have investigated. In Section II, we present our work on the detection of small molecules in both the liquid and vapor phase and the molecular recognition signatures which we have collected in those experiments. In Section III, we present our data on the liquid phase detection of proteins. Finally, in Section IV, we present our theoretical work, which is directed toward a further understanding of the signatures in the context of the molecular structure changes that the antibody–antigen complex may be undergoing during the molecular recognition process.

II. DETECTION OF SMALL MOLECULES

A. Vapor Phase Detection

It is well understood that for antibodies or other biomolecules to maintain their tertiary (three-dimensional) structure and hence their prescribed functionality, they must operate in an aqueous environment. This knowledge has led to the use of biomolecules for molecular recognition almost exclusively in the liquid phase. However, as is the case with home pregnancy test kits and bacterial test kits, the antibodies are immobilized in a preservative film.

If biomolecules can be utilized for the detection of specific analytes in the vapor phase, a powerful sensor can be developed capable of molecular recognition of airborne analytes of interest. In contrast, polymer films have relatively limited chemical specificity as compared with biomolecules. To date, there has been a limited amount of work reported on vapor phase biosensors. In a series of papers, Guilbault and fellow researchers [7]–[9] reported the use of films of biomolecules such as enzymes and antibodies on QCM devices for vapor phase detection of formaldehyde and organophosphorous pesticides such as parathion. Subsequent studies by others were unable to confirm the specificity reported by Guilbault. Rajakovic et al. [10] found that sensors coated with antiparathion antibodies showed sensitivities to malathion, parathion, and disulfoton that were not markedly different from the response of sensors coated with proteins (valproic acid antiserum, bovine serum albumin, and human IgG) containing no specific binding sites for these analytes. In addition, one could also conclude that the antiparathion QCM immunoassay sensor of
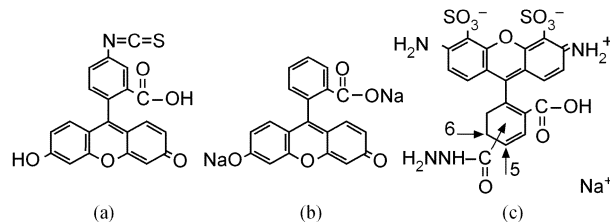

Fig. 1. Structural formulas for (a) FITC; (b) uranine; and (c) Alexa Fluor.

Ngeh-Ngwainbi et al. [8] does not indicate antigen-antibody binding activity. When an antigen–antibody binding event occurs, the antigen becomes tightly bound to the antibody and one would expect a shift in the baseline frequency of an acoustic-based oscillator. No such baseline shift was reported by Ngeh-Ngwainbi et al. [8]. One explanation for the nonspecific binding [11] was that in the absence of an aqueous environment, the binding sites on the antibodies will lose their prescribed structure required for molecular recognition.

1) Fluorescent Immunoassay Protocol: It is clear that the experimental protocol for gas phase biosensors should include, at least at the early stages of sensor development, an independent assessment of the predicted molecular recognition event. In light of this we have developed a novel fluorescent antibody/analyte assay. Further, to ensure hydration of the biomolecule, we have developed a method for applying a hydrogel layer over the immobilized antibodies.

A novel fluorescent immunoassay protocol was developed to provide a method, independent of the surface acoustic wave (SAW) device response, to confirm the occurrence of molecular recognition. SAW devices with and without anti-FITC antibody films were tested against two different fluorescent analytes: uranine and Alexa Fluor. The latter is hereafter referred to as Alexa. Our protocol consisted of presenting the analyte to the SAW resonator devices by bubbling nitrogen through a 1-nM aqueous solution of the analyte compound. After brief exposure to the analyte vapor, packaged devices were pulled from the system, washed with buffer to remove unbound analyte, and then viewed using the Zeiss LSM510 confocal fluorescent microscope (CLSM). The approximate time between exposure to the analyte and observation with the CLSM was 30 min. If fluorescence was observed in the CLSM image, this was taken as evidence of tightly bound fluorescent analyte.

For such an immunoassay, one would ordinarily choose fluorescein isothiocyanate (FITC) as the analyte, the structural formula of which is shown in Fig. 1(a). Our concern, however, was that because FITC is not water soluble, we would have to use an organic solvent which, during testing, might denature the immobilized antibodies. For this reason we selected uranine (a.k.a. fluorescein sodium salt) which is water soluble as the analyte for presentation to the FITC antibodies. The structural formula for uranine is presented in Fig. 1(b). It should be noted that, at the neutral pH we used for the uranine solution, the Na$^+$ ions will be dissociated from the molecule. In a similar pH range, the FITC mol-
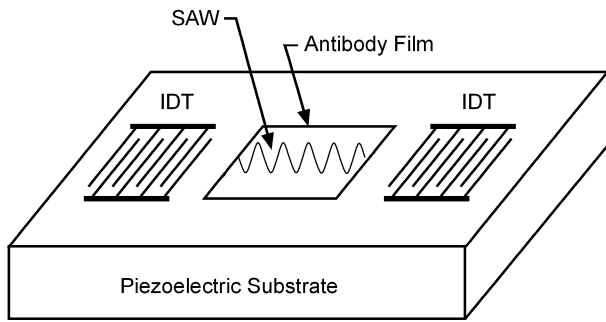
Fig. 2. SAW immunoassay sensor—delay line form.

Fig. 3. SAW resonator response to uranine vapor.

Fig. 4. SAW resonator response to Alexa.

ecule will lose the hydrogen atoms attached to the hydroxyl and carboxyl groups. Under these conditions, the uranine and FITC molecules would be identical with the exception of the isothiocyanate group on the FITC molecule. As you will see, in the results to be presented, we observed good binding affinity of the uranine molecule to the anti-FITC antibody, which, among other things, indicates that the isothiocyanate group is not important for antigen recognition by this particular anti-FITC antibody.

As in any immunoassay technique, it is important to test the device against an analyte which is dissimilar in substantive, but not radical, ways from the antigen. For this we have chosen Alexa, the structural formula for which is shown in Fig. 1(c), as the negative control. This compound is similar to FITC in that it has four linked phenyl groups, but the introduction of charged groups attached to the outer portion of the molecule prevents recognition by the anti-FITC antibody.

The data presented in the next section were generated from three SAW resonator sensors. The SAW devices differed only in the nature of the film coated onto the surface of the device. The anti-FITC device was coated with FITC antibody and the hydrogel layer. The uncoated device had just the hydrogel layer. "Uncoated" here refers to the absence of antibodies. The reference device had no coatings at all. In every other way, the SAW devices were identical.

2) Uranine Versus Alexa: Our approach was to construct a vapor phase biosensor by immobilizing a monolayer of antibodies onto the surface of a 250-MHz SAW device fabricated on ST-Quartz. For the particular cut and propagation direction, the interdigitated transducer on the device generates a Rayleigh which has particle polarization in the saggital plane that is retrograde and decays within roughly one acoustic wavelength from the surface. With our SAW devices, we have obtained sensitivities of approximately 20 Hz/pg with a detection limit on the order of a few picograms. To illustrate the sensing mechanism, we show a simple version of this device structure, a SAW delay line, in Fig. 2. In general, the device is then connected into an oscillator circuit, and the frequency of oscillation can be measured with great precision. When the antigen binds to the antibody, the acoustic velocity is decreased, and the oscillator frequency shifts to a lower value. The situation is much more complicated, however, when SAW resonators are used. Because a binding event might take place in either the reflector gratings or the transducer sections of the device, the frequency
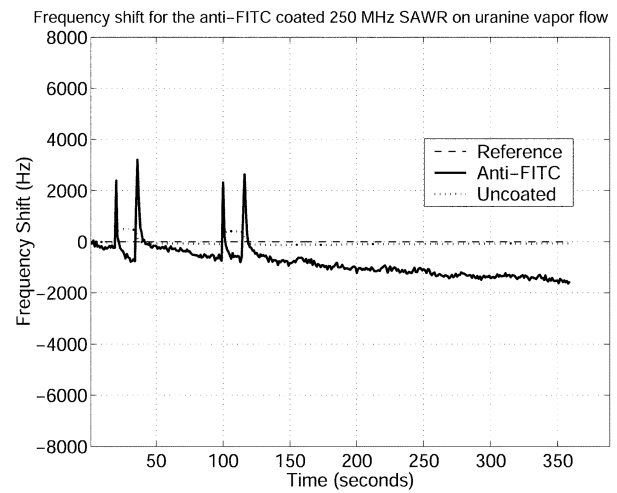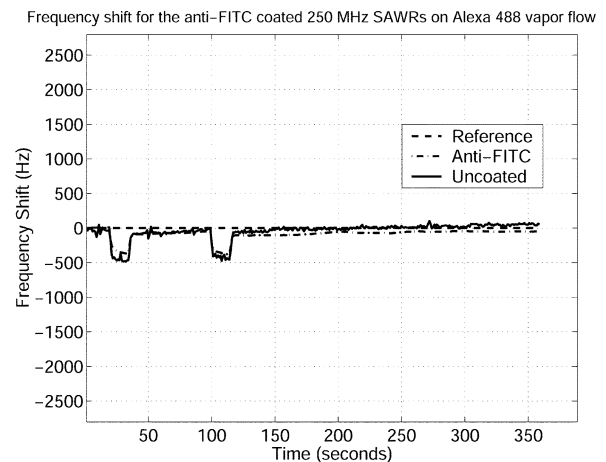
can increase or decrease in the presence of a binding event. To add to the confusion for SAW resonator signatures, stiffness changes in the biofilm would increase the resonant frequency of a delay line SAW sensor but could either increase or decrease the frequency of a SAW resonator.

Once we immobilized the anti-FITC onto a SAW resonator under test using protein-A, brief pulses of analyte vapor were flowed past the devices. The response of a reference device and oscillator circuit taken simultaneously with the response from the coated SAW resonators has already been subtracted from the recorded responses presented. The reference device is subjected to the same temperature environment as the sensor under test, but is not exposed to the analyte stream. The sensor data in the figures have already had the reference variation subtracted out; this resultant frequency shift was measured and recorded. Over numerous trials with coated and uncoated devices, a consistent picture began to emerge. In short, antigen–antibody binding occurred quickly and with a response far more dramatic than what was observed when the device was not coated with antibodies. For devices without antibodies, there was not a dramatic response and no baseline frequency shift. Two characteristic responses are presented in Figs. 3 and 4. As mentioned previously, for
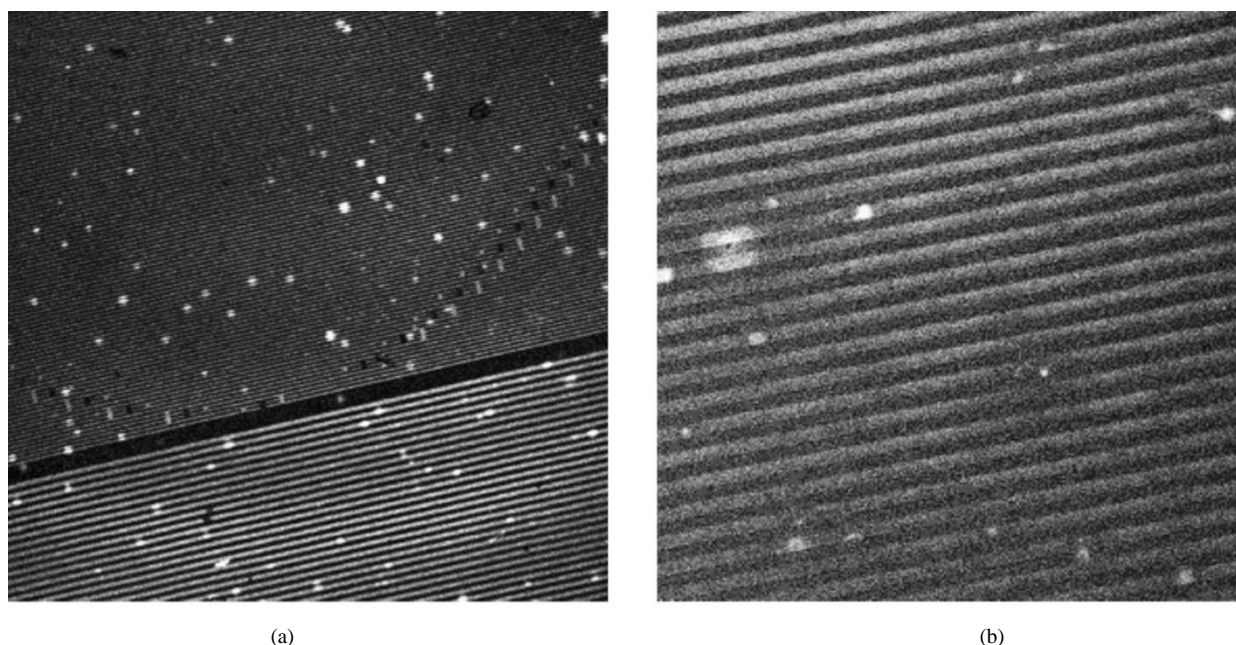
Fig. 5. CLSM image of anti-FITC/hydrogel-coated SAW chip after exposure to uranine vapor.

analyte presentation, N_2 gas was bubbled through a 1 nM solution of the analyte at a flow rate of 0.5 standard liters per minute (SLPM). The flow was continuous during the experiment. Vapor samples were extracted from the stream for two different 15–s periods (20–35 s and 100–115 s). In Fig. 3, we present the response of an anti-FITC coated device and an uncoated device to uranine vapor. As seen, the uncoated device shows a frequency shift during the sampling periods of a few hundred hertz and then returns to the baseline. This is a typical response for an uncoated device, and the return to baseline indicates that little of the analyte has permanently attached itself to the surface of the SAW device. For the anti-FITC coated device, the device shows a more radical frequency response and a fairly substantial shift in the baseline frequency. We believe that the more or less permanent shift in the baseline frequency represents direct evidence of molecular recognition in the vapor phase. One should keep in mind that the response shown is the raw data from the system and represents the frequency of the SAW resonator in the oscillator circuit. The oscillation frequency is determined by adequate loop gain and a 2π phase matching condition. Unfortunately, this does not always translate into a smooth, continuous curve, particularly if the phase of the resonator is near a discontinuous part of its transfer function response. Further it should be noted that the anti-FITC coated device had a substantially increased insertion loss over the uncoated device and hence, in this oscillator circuit, exhibits greater frequency noise. The steady decrease in the absence of the uranine pulse could be due to the fact that we continuously have uranine vapor flowing through a tube from which the vapor is extracted. We have not eliminated the possibility of diffusion of the analyte into the sensor chamber. The response of the uncoated sensor indicates a change in pressure associated with the introduction of the uranine analyte stream. Again, as stated previously, it is the magnitude

and time course of the frequency deviation which is relevant, since the complex nature of the SAW resonator makes it difficult to extract any pertinent information from the positive or negative direction of the frequency variation.

In Fig. 4, we show the response of an anti-FITC coated SAW resonator and an uncoated SAW resonator to the Alexa vapor. Neither of the devices shows a dramatic response to the analyte, and both the uncoated device and the anti-FITC coated device show no evidence of a marked baseline shift. This would indicate there is no binding of the Alexa to either of the device surfaces.

As indicated previously, in order to verify vapor phase analyte binding events, we developed a fluorescent antibody/analyte assay. After brief vapor phase exposure to the fluorescent analytes uranine and Alexa, the TO-8 packaged devices were pulled from the system, washed with buffer to remove unbound analyte and then viewed using a Zeiss LSM510 confocal fluorescent microscope (CLSM) located in the Institute for Bioengineering and Biosciences on Georgia Tech's campus. There were approximately 30 min between the presentation of the analyte and the capture of the CLSM image. If fluorescence was observed in the CLSM image, this was taken of evidence of tightly bound fluorescent analyte.

Many measurements have been taken, but only a small sampling of these will be presented here. Though it is not shown here, in the CLSM image for a hydrogel-coated SAW device exposed to uranine vapor, there was no evidence of fluorescence. In Fig. 5(a) and 5(b), we show CLSM images at $20\times$ and $40\times$ magnification, respectively, of an anti-FITC coated SAW chip after exposure to uranine. In this image, the bright spots are the fluorescent areas, indicating that over this relatively brief exposure to the uranine vapor, binding indeed occur. It should also be noted that fluorescent spots, as seen at the higher magnification, are predominantly located
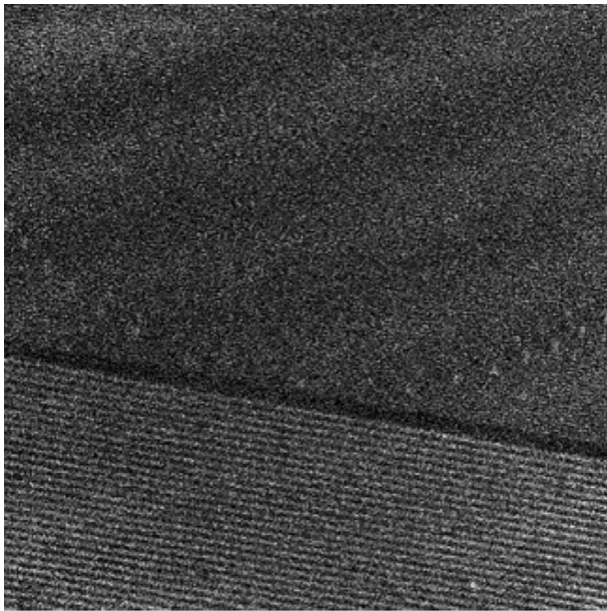
Fig. 6. CLSM image of anti-FITC/hydrogel-coated SAW chip after exposure to Alexa vapor.

Fig. 7. Antibody-coated and gel-coated device response to INEL vapor generator.

on the electrodes and not on the quartz. This observation supports the established notion that, using the conventional, previously presented protocol, the complex of antibody/protein-A molecules will be immobilized onto the gold electrodes.

Because we observed binding of uranine to anti-FITC, we were compelled to prove, in general, that we were observing molecular recognition, i.e., highly specific binding, by the antibodies. In this way, we could demonstrate that we are on the way to developing viable immunoassay for a vapor phase biosensor. To accomplish this, an aqueous solution of Alexa was used, which has a similar chemical structure (i.e., fluorescein moeity), but in theory should not bind to anti-FITC. In Alexa, the presence of negatively charged sulfite groups significantly changes the binding characteristics of the molecule. In Fig. 6, we show the CLSM image for the anti-FITC devices after exposure to Alexa and subsequent washing to remove unbound analyte. There is no evidence of fluorescence in these images, indicating that the Alexa did not bind to anti-FITC.

3) Cocaine Detection: The highly specific and complex nature of olfactory sensing systems has over the past decade inspired researchers to the development of vapor phase chemical detection systems which go by the name of "electronic noses." These devices and systems are currently being used in biotechnology, food industry, medicine, environment, and most recently law enforcement applications. Interdiction efforts continue in the search for technologies which can provide an inexpensive alternative to dogs as detectors of narcotics and explosives. One of the principal motivations for development of electronic noses for these applications is the expense associated with of the handlers and training and care for the dogs. Further, it is still unclear as to what chemically the dogs are actually detecting, and this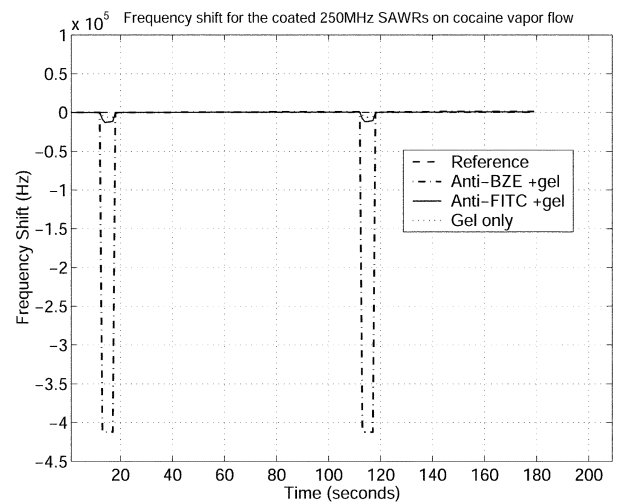 may vary from dog to dog. Consequently, not all dogs do respond to the same cocaine sample. Although the dogs have proved to be a highly useful tool in detecting illicit materials, as a tool for analytical chemistry they leave one wanting. One would never accept data from an instrument without having a solid idea of the physical mechanism behind a detection event.

For these experiments, we used both anti-FITC coated and hydrogel-coated devices as negative controls and immobilized antibodies for benzoylecgonine (BZE) for positive detection of cocaine. BZE is a metabolic breakdown product of cocaine, but differs only slightly from cocaine. The location of this difference does not appear to be a part of the epitope recognized by anti-BZE. One motivation for using anti-FITC as a negative control is that FITC and BZE both have molecular weights in the range of 300 Da. In addition, the two molecules may both possess a hydrophobic epitope.

Using anti-BZE antibodies immobilized onto SAW resonators, we were able to consistently detect cocaine vapors presented using the Idaho National Engineering Laboratories (INEL) vapor generator designed specifically for the purpose of testing analytical equipment. In Fig. 7, we present the response of anti-FITC, anti-BZE, and hydrogel-only sensors to a 1-ng pulse of cocaine over 5-s intervals. The pulse was injected into a constant flow of 180 cubic centimeters per minute (ccm) to minimize the impact associated with a sudden pressure differential. The anti-BZE device has a far more dramatic instantaneous response than the anti-FITC device. Note also that there is little or no difference between the gel-only and anti-FITC device responses. This characteristic response was found to be independent of the SAW resonator device location within the sensor head which holds and facilitates the simultaneous sampling of four sensors. During the pulse cycles, we obtained a consistent relationship between the sequence and the amount of frequency shift (Δf) on the presentation of cocaine vapor.

Δf(during pulse cycle): Uncoated < Gel only

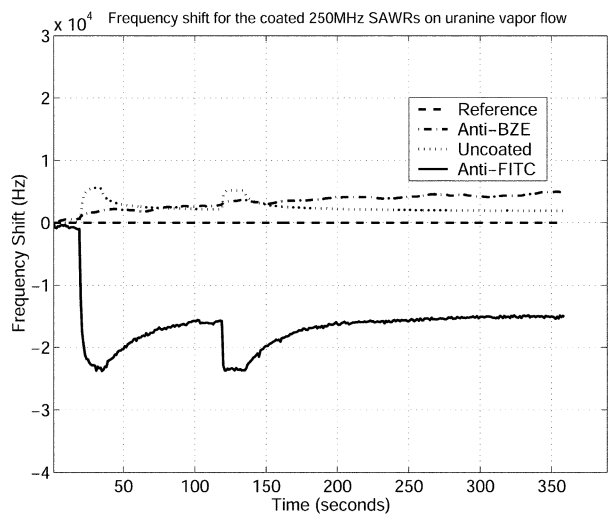$$< \text{Anti-FITC/gel} \ll \text{Anti-BZE/gel}$$
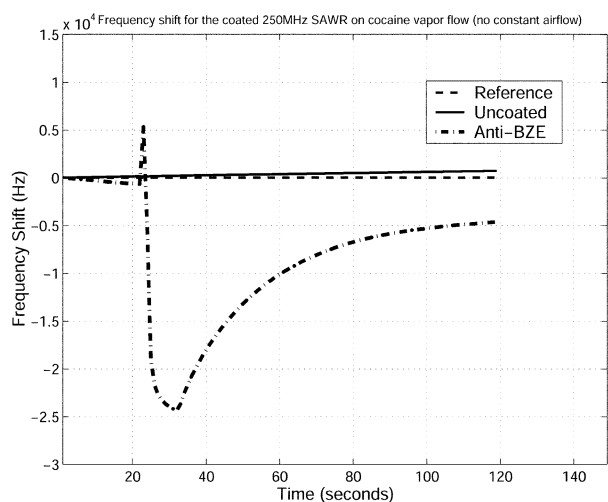
Fig. 8. Antibody-coated devices response to uranine.

Fig. 9. SAW resonator device response to pulse of cocaine from INEL vapor generator under nonconstant airflow conditions.

Fig. 10. SAW resonator device response to air drawn from the head space over a vial of crack cocaine.

Our findings suggest that during the pulse cycles, the differences in the magnitude of the frequency shift between anti-BZE and other sensors are significant. This fact may be utilized for the establishment of a decision criterion for the real time cocaine detection.

As a control, we subjected antibody coated devices to a vapor sample supplied by bubbling N_2 through a 1-nM solution of uranine. In Fig. 8, we show these results. The frequency shift during the exposure to uranine was very dramatic for the anti-FITC coated device, and only a slight response for the anti-BZE device is observed. In Fig. 9, we present the response of an anti-BZE coated device to a 10-s 1-ng pulse of cocaine from the INEL vapor generator under nonconstant flow conditions. A distinct difference here from the response shown in Fig. 7 is that there is a more gradual decay of the response after the presentation of the pulse. For this "nonconstant flow" measurement, a pulse of cocaine vapor is injected into the sensor head for 10 s, and then the unbound sample exits from the sensor head only by diffusion. This essentially increases the probability that
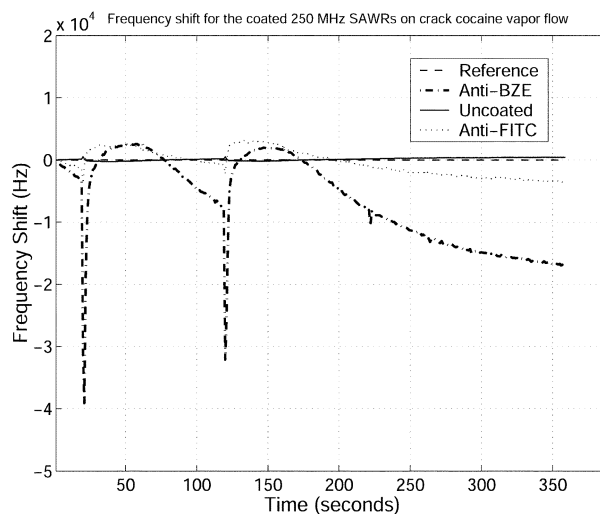
more of the cocaine molecules will become bound to the anti-BZE antibodies. For the constant flow case (see Fig. 7), any cocaine molecules left unbound after the 10-s pulse are likely to be swept out of the sensor head by the 200-ccm flow.

In collaboration with the Georgia Bureau of Investigation (GBI) chemical analysis scientists, we investigated the headspace over a seized sample being processed. We presented a sample of vapor to the SAW sensor head. The sample was believed to be cocaine freebase, commonly called crack. In Fig. 10, we present the response of the sensors to a sample drawn from the headspace. This analysis revealed the device characteristic that we had previously observed under laboratory conditions using the INEL vapor generator, namely, a sharp, dramatic initial transient when the sample is drawn into the sensor head and the exponential decay to a shifted baseline. This is what we have consistently taken to be evidence of molecular recognition of the target analyte. In essence, this is the signature $\Delta f(t)$. This signature consists of a sharp initial transient followed by a baseline shift. As a control, we used anti-FITC antibodies with the sample of crack cocaine and no such dramatic response was observed. This response was only observed when the sample was taken directly from the headspace. The characteristic response, we believe, is determined not only by device design but also by the molecular recognition event taking place between the antibody and its antigen. That is, we believe that the initial transient observed is due to mass loading and some changes in the spring constant of the biofilm. Our studies suggest that BZE, a cocaine metabolite usually the target of cocaine urine tests, may possess a similar epitope to that of a cocaine molecule.

B. Liquid Phase Detection of Small Molecules

The ST-Quartz Rayleigh wave devices which we utilized for the vapor phase biosensor measurements are not suitable for liquid phase measurements, so in order to map our protocol over to liquid phase measurements, we utilized

10-MHz commercially available QCM devices. We recorded the $\Delta f(t)$. In addition, the flow cell which we constructed was composed of two sensors, one coated with an antibody specific for the target analyte and another uncoated device as a reference sensor.

Acoustic sensors represent an approach for high-precision sensing, which has been highly successful and which has a long history of reduction to practice. QCMs were there at the dawn of the semiconductor industry, having been utilized since the 1950s [1] to monitor the thickness of metals being deposited on wafers in evaporation systems. In these early papers and in later papers, it was pointed out that it was not just the mass which induced the change in the resonant frequency of the crystal, but that there are other factors that affect the resonant frequency as well [12]–[14]. In fact, in addition to mass, QCMs are sensitive to viscosity, charge, and the mechanical characteristics of the chemically selective film immobilized on the device surface. It is interesting to note that at least as far back as Mason [15] in 1948 that shear vibrating crystals could be used to measure viscosity and shear elasticity in liquids.

We will assume that our reference sensor is close to the active sensor, and hence assume that it samples essentially the same volume as the active sensor. As such, we will presuppose that the charge and viscosity effects will be roughly identical on the two sensors, so that the only difference between them will be the molecular recognition event is taking place on the active sensor and that this recognition event is not taking place on the reference sensor. The difference in resonant frequencies between the two sensors will then be due strictly to the impact of the molecular recognition event, which will be both mass attachment and any induced changes in the mechanical characteristics of the chemically sensitive film.

Because we gather real-time data, we can monitor the resonant frequency changes of the QCM before, during, and after the molecular recognition event. We will make the assumption that the additional mass on the sensor, relative to the reference sensor, is due strictly to the antigen which has bound to its immobilized antibody. Further, we will make the somewhat radical conjecture that the changes in the mechanical properties of the film are due to conformational changes in the immobilized antibodies.

A dual differential QCM system was designed to detect increasing concentrations of uranine, a small fluorescent molecule ($\sim$300 Da), in blood sera. Addition of the nanomolar concentrations of uranine to the flow cell resulted in an initial transient response and an upward shift in the baseline. The response was filtered from the usual fluid disturbance shifts using a reference crystal.

Using a dual sensor system, we were able to observe results of adding 100 μl of a nanomolar solution of uranine to a 4:3(v/v)mixture of serum to Tris-acetate/EDTA (TAE) buffer. The reference crystal was prepared in the same fashion as the antiuranine coated sensor, which used an alkane-thiol attachment protocol. Both sensors were fitted to a flow cell that allowed only one side of each crystal to be exposed to the liquid. Careful addition of 100 μl of
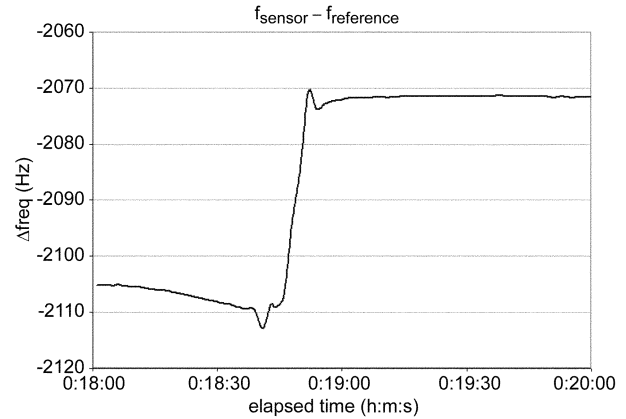

Fig. 11. QCM difference frequency plot showing response during addition of 100-μL uranine to 700 μL of blood sera.

1-nM concentration of uranine followed by monitoring of the initial transient and subsequent frequency change was recorded and a sample transient curve is presented in Fig. 11. This concentration, diluted from the nanomolar uranine, corresponds to a detection limit of less than 1 ppb, and this in the presence of perhaps thousands of complex proteins contained in the blood sera. Several things should be remembered about this particular experiment. One of these is that this represents the detection of a small molecule with a molecular weight in the range of 300 Da. Another is that the resonant frequency shifts *upward*. According to the Sauerbrey equation [1], which follows, mass loading should lower the resonant frequency:

$$\Delta f = -\frac{2f_o^2 \rho_s}{V_a \rho_r} \tag{1}$$

where Δf is the resonator frequency shift; f_o is the resonator center frequency; ρ_s is the mass density per m^2 of analyte attached to the surface; V_a is the acoustic wave velocity in the resonator; and ρ_r is the volume mass density of resonator material.

Based on our derivation, presented later in this paper, we hypothesize that a stiffening of the biofilm during and after the molecular molecular recognition event would give rise to an increase in resonant frequency, i.e., a positive Δf shift.

These data hint at one of the intriguing aspects of signature collection. One of the troubling aspects that plagues biosensor technology is the so-called nonspecific binding; that is to say, the sensor responds to molecules which stick to the surface of the biosensor independent of the molecular recognition event we seek to observe. It is likely that many of the proteins in the blood sera are sticking to both the reference and the sensor, but the signature can readily be extracted from this otherwise background signal.

III. DETECTION OF PROTEINS

We have done a limited amount of work in the area of signal extraction from protein binding experiments, and that has been with a biomarker related to plant development. Calmodulin is a plant protein significant for its role as a
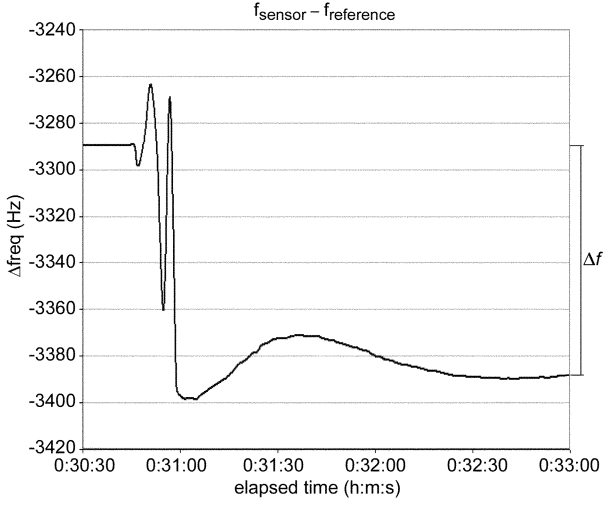
Fig. 12. QCM immunosensor transient response to calmodulin.

biomarker in embryonic development of seedlings. The active sensor in this case had an anticalmodulin antibody immobilized on the surface, and 100 μl of 5 μg/ml calmodulin was added to the TAE buffered solution. This represents the introduction of 500 ng of calmodulin into the reservoir. The resulting transient QCM response is shown in Fig. 12. Note that in contrast to the uranine-anti-FITC experiment, the net frequency shift is downward, indicating the predominance of mass loading over mechanical stiffness increase in the film. Also, that there is quite a bit of character in this signature—overshoot and ringing followed by an asymptotic approach to a baseline shifted by Δf.

IV. THEORETICAL UNDERPINNINGS VIA TIME-DEPENDENT PERTURBATION THEORY

In this section, we present a broad derivation using time-dependent perturbation theory to go beyond the static Sauerbrey equation to a more dynamic equation which can be used to evaluate our molecular recognition signatures. We will begin with the reciprocity relation of Auld [16]

$$\nabla \cdot \left[-v_u^* \cdot T_p - v_p \cdot T_u^* + \varphi_u^* \frac{\partial D_p}{\partial t} + \varphi_p \frac{\partial D_u^*}{\partial t} \right]$$
$$= -\frac{\partial}{\partial t} \left([v_u^* \; T_u^* - \nabla \varphi_u^*] \begin{bmatrix} \rho & 0 & 0 \\ 0 & : s :^E & : d \cdot \\ 0 & \cdot d : & \cdot \in \cdot^T \end{bmatrix} \right.$$
$$\left. \times \begin{bmatrix} v_p \\ T_p \\ -\nabla \varphi_p^* \end{bmatrix} \right) + (v_u^* \cdot F_p + v_p \cdot F_u^*)$$
$$+ \varphi_u^* \frac{\partial \rho_{ep}}{\partial t} + \varphi_p \frac{\partial \rho_{eu}^*}{\partial t}$$

where superscript "u" denotes state variables of the unperturbed field; superscript "p" denotes state variables of the perturbed field; v is the particle velocity vector; T is the stress tensor; D is the electric field displacement vector; φ is the electrostatic potential; F is the external mechanical body force; and ρ_e volume density of mobile charge carriers.

In this analysis, we will maintain our focus on the predominant mechanical perturbations, which means that we will neglect the terms related to the electrostatic potential and displacement and the influence of mobile carriers. For the experimental data we present, this assumption is justified because we are using weakly piezoelectric quartz crystals as the sensor material. Beyond this, we are also assuming the utilization of a reference sensor, also coated with a biomolecule such as an antibody, not specific for the analyte of interest. In this, the secondary impact of ionic charge carriers in the solution over the sensor as well as the fluid viscosity will be canceled out via subtraction of the oscillation frequency of each of the sensors. Keep in mind that with our current experimental system, we can collect data at most 300 times per minute, giving an intersample time of 200 ms. Given the nominal resonant frequency of 10 MHz, the differential effects of charge and viscosity will be averaged over 2 million cycles of oscillation.

In addition, we will assume that the external body force term can be neglected. This leaves us with

$$\nabla \cdot [-v_u^* \cdot T_p - v_p \cdot T_u^*]$$
$$= -\frac{\partial}{\partial t} \left\{ [v_u^* \; T_u^*] \begin{bmatrix} \rho & 0 \\ 0 & : s :^E \end{bmatrix} \begin{bmatrix} v_p \\ T_p \end{bmatrix} \right\}. \quad (2)$$

We must now consider that for the case of the biofilm, we are dealing with the perturbation of the material parameters ρ and s^E, and, as we will assert later on, we will allow these material parameters to vary with time. The right side of (2) then becomes

$$-\left\{ \frac{\partial}{\partial t} \left([v_u^* \; T_u^*] \begin{bmatrix} \rho_u & 0 \\ 0 & : s_u :^E \end{bmatrix} \right) \begin{bmatrix} v_p \\ T_p \end{bmatrix} \right.$$
$$\left. + [v_u^* \; T_u^*] \frac{\partial}{\partial t} \left(\begin{bmatrix} \rho_p & 0 \\ 0 & : s_p :^E \end{bmatrix} \begin{bmatrix} v_p \\ T_p \end{bmatrix} \right) \right\} \quad (3)$$

where ρ_u is the density of unperturbed case, i.e., when the antibody film is present but is not bound to its antigen; ρ_p is the mass density of perturbed case, i.e., antibody film when some of the antigen has bound to the antibody; s_u^E is the compliance tensor for the unperturbed case; and s_P^E is the compliance tensor for the perturbed case. Also be mindful that the unperturbed resonant frequency ω_u is time independent but that the perturbed resonant frequency ω_p is in fact time dependent. Expanding (3), we will have

$$i\omega_u [v_u^* T_u^*] \begin{bmatrix} \rho_u & 0 \\ 0 & : s_u :^E \end{bmatrix} \begin{bmatrix} v_p \\ T_p \end{bmatrix}$$
$$- i\omega_p [v_u^* T_u^*] \begin{bmatrix} \rho_p & 0 \\ 0 & : s_p :^E \end{bmatrix} \begin{bmatrix} v_p \\ T_p \end{bmatrix}$$
$$- it \frac{\partial \omega_p}{\partial t} [v_u^* T_u^*] \begin{bmatrix} \rho_p & 0 \\ 0 & : s_p :^E \end{bmatrix} \begin{bmatrix} v_p \\ T_p \end{bmatrix}$$
$$- \left\{ [v_u^* T_u^*] \begin{bmatrix} \frac{\partial \Delta \rho}{\partial t} & 0 \\ 0 & \frac{\partial : \Delta : s :^E}{\partial t} \end{bmatrix} \begin{bmatrix} v_p \\ T_p \end{bmatrix} \right\}. \quad (4)$$

If we let

$$\Delta \omega = \omega_p - \omega_u$$

it is helpful to recognize that

$$\frac{\partial \omega_p}{\partial t} = \frac{\partial \Delta \omega}{\partial t}$$

since ω_u does not vary with time.

Equation (4) can be rewritten as

$$-i\Delta\omega[v_u^* T_u^*]\begin{bmatrix} \rho_u & 0 \\ 0 & :s_u :^E \end{bmatrix}\begin{bmatrix} v_p \\ T_p \end{bmatrix}$$
$$- i\omega_u[v_u^* T_u^*]\begin{bmatrix} \Delta\rho & 0 \\ 0 & :\Delta s :^E \end{bmatrix}\begin{bmatrix} v_p \\ T_p \end{bmatrix}$$
$$- it\frac{\partial \Delta\omega}{\partial t}[v_u^* T_u^*]\begin{bmatrix} \rho_u & 0 \\ 0 & :s_u :^E \end{bmatrix}\begin{bmatrix} v_p \\ T_p \end{bmatrix}$$
$$- it\frac{\partial \Delta\omega}{\partial t}[v_u^* T_u^*]\begin{bmatrix} \Delta\rho & 0 \\ 0 & :\Delta : s :^E \end{bmatrix}\begin{bmatrix} v_p \\ T_p \end{bmatrix}$$
$$- \left\{[v_u^* T_u^*]\begin{bmatrix} \frac{\partial \Delta\rho}{\partial t} & 0 \\ 0 & \frac{\partial:\Delta:s:^E}{\partial t} \end{bmatrix}\begin{bmatrix} v_p \\ T_p \end{bmatrix}\right\}.$$

If we let

$$\Re = [v_u^* T_u^*]\begin{bmatrix} \Delta p & 0 \\ 0 & :\Delta s :^E \end{bmatrix}\begin{bmatrix} v_p \\ T_p \end{bmatrix}$$

then (4) can be rewritten more compactly, yielding the more concise form for (2) of

$$\nabla \cdot [-v_u^* \cdot T_p - v_p \cdot T_u^*]$$
$$= -i\Delta\omega[v_u^* T_u^*]\begin{bmatrix} \rho_u & 0 \\ 0 & :s_u :^E \end{bmatrix}\begin{bmatrix} v_p \\ T_p \end{bmatrix}$$
$$- i\omega_u\Re - it\frac{\partial \Delta\omega}{\partial t}[v_u^* T_u^*]\begin{bmatrix} \rho_u & 0 \\ 0 & :s_u :^E \end{bmatrix}\begin{bmatrix} v_p \\ T_p \end{bmatrix}$$
$$it\frac{\partial \Delta\omega}{\partial t}\Re - [v_u^* T_u^*]\begin{bmatrix} \frac{\partial \Delta\rho}{\partial t} & 0 \\ 0 & \frac{\partial:\Delta:s:^E}{\partial t} \end{bmatrix}\begin{bmatrix} v_p \\ T_p \end{bmatrix}. \quad (5)$$

Equation (6) represents the fundamental partial differential equation which could be applied generally to various resonator configurations such as SAW, flexural plate wave (FPW), surface transverse wave (STW) resonators, to name a few. The details of utilization of this PDE from this point forward hinges on the specific embodiment of the resonator. As a simple and analytically tractable case, we will treat the case of the QCM resonator which we have used in the collection of the data presented previously.

The next issue is to establish the assumptions for solution of the perturbation problem, i.e., to presume what is being perturbed. Here we will, after the approach taken in Auld [16], assume that the spatial distribution of the acoustic fields will be unchanged but that the resonant frequencies will be perturbed.

That is to say that we will have

$$v_u = v(x,y,z)e^{i\omega_u t}$$
$$T_u = T(x,y,z)e^{i\omega_u t}$$
$$v_p = v(x,y,z)e^{i\omega_p t}$$
$$T_p = T(x,y,z)e^{i\omega_p t}. \quad (6)$$

For the QCM on AT-cut quartz, we will take the y direction as the axis through the thickness of the crystal and the x axis as the direction associated with acoustic field particle

velocity. The fields presented in (4) will become more precisely for this case

$$v_u = v_x(y)e^{i\omega_u t}\hat{x}$$
$$T_u = c_{44}S_{xy} = \frac{c_{44}}{i\omega_u}\frac{\partial v_x}{\partial y}e^{i\omega_u t}$$
$$v_p = v_x(y)e^{i\omega_p t}\hat{x}$$
$$T_p = c_{44}S_{xy} = \frac{c_{44}}{i\omega_u}\frac{\partial v_x}{\partial y}e^{i\omega_p t}. \quad (7)$$

This greatly simplifies the complexity of the problem in that we no longer must keep track of vectors and tensors for the acoustic field but essentially scalars for the particle velocities and stress tensors. We can now move onto the further reduction of complexity of the partial differential equation of (5).

The next step will be to integrate both sides of the equation over the volume of the resonator, evaluating these integrals term by term. Applying the divergence theorem the first term of (5) yields

$$\int (\nabla \cdot [-v_u^* \cdot T_p - v_p \cdot T_u^*]) \, dV$$
$$= \oint [-v_u^* \cdot T_p - v_p \cdot T_u^*] \cdot d\vec{S}. \quad (8)$$

Let us consider the special case of a QCM sensing in either a vapor or a liquid. These media are considered fluids in the sense that neither will support a shear wave. Hence, the boundary condition at the surfaces of the QCM is the so-called stress-free boundary condition, i.e., $T \cdot \hat{n} = \vec{0}$. This is not precisely the case for a viscous fluid, but as an initial cut at developing the time-dependent perturbation theory, it is the one which we will use. Under the stress-free boundary conditions, the surface integral of (8) is zero.

Integrating the first term on the right side of (5), we have

$$\int -i\Delta\omega \left\{[v_u^* T_u^*]\begin{bmatrix} \rho_u & 0 \\ 0 & :s_u :^E \end{bmatrix}\begin{bmatrix} v_p \\ T_p \end{bmatrix}\right\} dV = -i4\Delta\omega U$$
$$(9)$$

where U is the total energy stored in the unperturbed field. Next we integrate $\Re$ over the volume

$$\int \Re \, dV = \int [v_u^* T_u^*]\begin{bmatrix} \Delta\rho & 0 \\ 0 & :\Delta s :^E \end{bmatrix}\begin{bmatrix} v_p \\ T_p \end{bmatrix} dV$$
$$= \int (\Delta\rho v_u^* \cdot v_p + T_u^* : \Delta s :^E T_p) \, dV. \quad (10)$$

Through utilization of the constitutive relations for stress and strain, the second term in the integrand of (10) can be rewritten as $-S_u^* : \Delta c :^E S_p$. It is prudent at this point to look further at what is meant by Δc^E and $\Delta\rho$. Note that this perturbation in the material parameters is

$$\Delta\rho = \rho_p - \rho_u$$
$$\Delta c^E = c_p^E - c_u^E.$$

It is now time to simplify the tensor relationships of the derivation to date to deal strictly with the case of the QCM sensor. As can be seen from (7), the only term of the stiffness tensor which will be applicable to this problem is the c_{44}
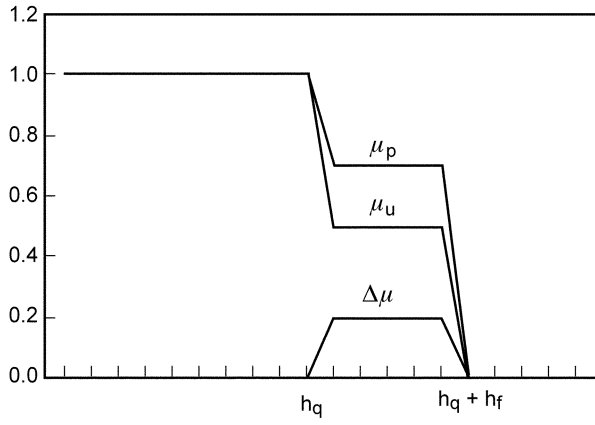
Fig. 13. Mechanical stiffness of biofilm.

term, which is also the Lame constant μ; as such, Δc^E will be written as $\Delta \mu$. In Fig. 13, we illustrate what we mean by $\Delta \mu$. In this figure, h_q is the thickness of the sensor, and h_f is the thickness of the biofilm immobilized onto the sensor surface. Because the biomolecular recognition activity only affects the biofilm, the $\Delta \mu$ term is nonzero only in the region of the biofilm, from h_q to $h_q + h_f$.

The volume integral of (10) will hence only be nonzero over the volume of the biomolecular layer. Further, since the biofilm is only a few hundred angstroms thick, we will assume that the acoustic field does not change over the volume of the biomolecular layer; we will thus express the particle velocity as v_{xo}, the unperturbed shear particle velocity at the surface of the QCM. Hence, the first term of (10) becomes

$$\iint dx\, dz \int_{h_q}^{h_q+h_f} \Delta \rho v_{xo}^2 \, dy = A \Delta \rho h_f v_{xo}^2$$

where $A = $ area of the smallest electrode on the QCM. Noting that the strain of the second term in (10) at the surface of the QCM is given by

$$S_{xyo} = \frac{1}{i\omega} \left. \frac{\partial v_x}{\partial y} \right|_{\text{surface}} = \frac{k_n}{i\omega} v_{xo}$$

where k_n is the wavenumber associated with the x-polarized shear wave. The volume integral of the second term in (10) then becomes

$$\iint dx\, dz \int_{h_q}^{h_q+h_f} \Delta \mu S_{xyo}^* S_{xyo} \, dy = A \Delta \mu h_f \frac{k_n^2}{\omega^2} v_{xo}^2$$
$$= \frac{A h_f \Delta \mu}{V_s^2} v_{xo}^2.$$

Putting the first and second terms together, (10) becomes

$$\int \Re \, dV = A h_f v_{xo}^2 \left[\Delta \rho - \frac{\Delta \mu}{V_s^2} \right]. \tag{11}$$

Extending this, we can quickly write the last term of (5) as

$$A h_f v_{xo}^2 \left[\frac{\partial \Delta \rho}{\partial t} - \frac{1}{V_s^2} \frac{\partial \Delta \mu}{\partial t} \right].$$

Combining these subterms, we will have

$$t \frac{\partial \Delta \omega}{\partial t} \left(1 + \frac{A h_f v_{xo}^2}{i 4U} \left[\Delta \rho - \frac{\Delta \mu}{V_s^2} \right] \right) + \Delta \omega = \frac{A h_f v_{xo}^2}{i 4U}$$
$$\times \left\{ -i\omega_u \left[\Delta \rho - \frac{\Delta \mu}{V_s^2} \right] + \left[\frac{\partial \Delta \rho}{\partial t} - \frac{1}{V_s^2} \frac{\partial \Delta \mu}{\partial t} \right] \right\}. \tag{12}$$

The second term in the derivative of $\Delta \omega$ can be neglected, as it is much, much smaller than one. By noting that

$$4U = \rho_q h_q v_{xo}^2 A$$

we can rewrite the term in front of the right side of (12) as

$$\frac{2 f_u}{\sqrt{\rho_q \mu_q}}.$$

This will yield a differential equation for $\Delta \omega$ of

$$t \frac{\partial \Delta \omega}{\partial t} + \Delta \omega = \frac{\omega_u h_f}{\pi \sqrt{\rho_q \mu_q}} \left\{ -\omega_u \left[\Delta \rho - \frac{\Delta \mu}{V_s^2} \right] \right.$$
$$\left. + i \left[\frac{\partial \Delta \rho}{\partial t} - \frac{1}{V_s^2} \frac{\partial \Delta \mu}{\partial t} \right] \right\}. \tag{13}$$

As a simple check of the derivation, let us assume that neither $\Delta \omega, \Delta \rho$, or $\Delta \mu$ changes with time. This will give us

$$\Delta \omega = -\frac{\omega_u^2 h_f}{\pi \sqrt{\rho_q \mu_q}} \left[\Delta \rho - \frac{\Delta \mu}{V_s^2} \right] \tag{14}$$

which is essentially the well-known Sauerbrey equation with a term added to include static changes in the mechanical stiffness of the film. This presentation also brings to light the notion that mass attaching to the sensor will lower the resonant frequency of the sensor, but a stiffness increase will actually increase the resonant frequency.

If one knew both $\Delta \rho$ and $\Delta \mu$ as functions of time, one could solve this differential equation. Though $\Delta \rho$ can be extracted from kinetic approximations, the variation in the stiffness $\Delta \mu$ is at present a complete unknown. X-ray crystallography represents perhaps the best chance at assessing the degree of conformational change due to a biomolecular interaction, this technique provides at best a measure to the structure of a biomolecule before and long after the molecular recognition event. Our hypothesis is that there is a conformational change associated with the molecular recognition event, and that by recording $\Delta \omega(t)$, we have a method to extract information regarding its occurrence.

If one in fact did know $\Delta \rho$ and $\Delta \mu$, (13) could be solved using the integrating factor method. Under this approach we would have

$$\Delta \omega = \frac{1}{t} \left(\int^t \frac{\omega_u h_f}{\pi \sqrt{\rho_q \mu_q}} \left\{ -\omega_u \left[\Delta \rho(\tau) - \frac{\Delta \mu(\tau)}{V_s^2} \right] \right\} d\tau \right.$$
$$\left. + i \left[\Delta \rho(t) - \frac{\Delta \mu(t)}{V_s^2} \right] + C \right) \tag{15}$$

where C is a constant to be utilized in satisfying the initial condition of a problem. In short, this equation represents a mathematical tool for extract conformational change data from real-time QCM measurements.

An independent case for conformational change during antibody–antigen interactions can be established by looking at the work of X-ray crystallographer I. Wilson. In a 1990

[17] paper in *Science*, Wilson first proposed that an antibody will undergo conformational changes before and during a molecular recognition event with its antigen or with "near recognition events" with molecules containing a similar, but not identical epitope. Further work by Wilson [18]–[21] revealed high-order ($\sim$10- 12 Å) conformational changes during specific and nonspecific antibody–antigen (specifically small molecules) interactions. In similar experiments involving larger molecules, such as proteins [21], there was very little conformational change in the antibody binding regions. The Complimentary determining region heavy chain 3 (CDR H3) as part of the six hypervariable loop CDR responsible for molecular recognition [18], was identified as the loop motif involved in the majority of conformational changes during a binding event, although the other loops did show some changes in the range of 1–2 A. This was discovered by comparing the crystal structures of unliganded antibody structures with that of the ligand bound structure. Wilson concluded that the rotation in the CDR H3 region was $15°$–$20°$ as a result of the binding event. Such range of motion eliminates the argument for a strictly lock and key mechanism proposed by Polijak [22] which requires a more rigid model. Biolayer rigidity—that is to say, the assumption that the biolayer is mechanically static—is the basis for strictly mass-loading interpretations of QCM sensor data using Sauerbrey analysis. It is clear from a combination of Wilson's work and our own that a QCM immunosensor requires considerations of both mass loading and conformational change as part of the device response. A further explanation of our data presented in Fig. 11 is that in this case of a small molecule, the conformational change in the immobilized antibodies is large when compared to the mass loading effect and thus, by (14), an increase in frequency. For proteins, our experimental results presented in Fig. 12 suggest that the impact of conformational change resulting from antibody–antigen binding is less than the effect of mass loading effect. This is evidenced by the large decrease in the resonant frequency after the binding event. This assertion is supported by evidence from crystallographic studies which shows surface interactions between the CDRs of the antibody binding fragment and the surface exposed regions of the protein being the predominant binding and requires minimal antibody structural changes based on the root mean square deviation between unliganded and ligand-bound models. The X-ray crystallography data of Wilson represents an evaluation of biomolecular structures before and after the binding event. The prospect exists to "observe" these conformational changes during the binding event using acoustic resonator sensors. Equation (15) provides a means by which the conformational change data given by the $\Delta\mu(t)$ signature can be extracted from the measured changes $\Delta\omega(t)$ in the resonant frequency.

V. Summary and Conclusion

In this paper, we have presented our recent results for vapor and liquid phase acoustic wave biosensors. In particular, we have taken a closer look at the signatures of these responses that we believe to be related to a molecular recognition event between antibody and antigen. Further, we have developed an equation based on time-dependent perturbation theory to aid in the future evaluation of these signatures. This theoretical work bolsters the case that there is important information which can be extracted from the signatures.

References

[1] G. Sauerbrey, " Use of quartz vibrator for weighing thin films on a microbalance," *Z. Phys.*, vol. 155, pp. 206–210, 1959.

[2] D. Diamond, Ed., *Principles of Chemical and Biological Sensors*. New York: Wiley, 1998.

[3] D. D. Stubbs, W. D. Hunt, S. H. Lee, and D. F. Doyle, "Gas phase activity of anti-FITC antibodies immobilized on a surface acoustic wave resonator device," *Biosens. Bioelectron.*, vol. 17, no. 6–7, pp. 471–477, June 2002.

[4] D. D. Stubbs, S. H. Lee, and W. D. Hunt, "Molecular recognition for electronic noses using surface acoustic wave immunoassay sensors," *IEEE Sensors J.*, vol. 2, pp. 294–300, Aug. 2002.

[5] ——, "Cocaine detection using surface acoustic wave immunoassay sensors," in *Proc. IEEE Int. Frequency Control Symp.*, 2002, pp. 289–293.

[6] G. Kohler and C. Milstein, "Continuous cultures of fused cells secreting antibody for predefined specificity," *Nature*, vol. 256, pp. 495–497, 1975.

[7] G. G. Guilbault, "Determination of formaldehyde with an enzyme-coated piezoelectric crystal detector," *Anal. Chem.*, vol. 55, pp. 1682–1684, 1983.

[8] J. Ngeh-Ngwainbi, P. H. Foley, S. S. Kuan, and G. G. Guilbault, "Parathion antibodies on piezoelectric crystals," *J. Am. Chem. Soc.*, vol. 108, pp. 5444–5447, 1986.

[9] G. G. Guilbault and J. H. Luong, "Gas phase biosensors," *J. Biotechnol.*, vol. 9, pp. 1–10, 1988.

[10] L. Rajakovic, V. Ghaemmaghami, and M. Thompson, "Adsorption on film-free and antibody-coated piezoelectric sensors," *Anal. Chem. Acta.*, vol. 207, p. 111, 1989.

[11] D. S. Ballantine, R. M. White, S. J. Martin, A. J. Ricco, E. T. Zellers, G. C. Frye, and H. Wohltjen, *Acoustic Wave Sensors: Theory, Design, and Physico-Chemical Applications*. New York: Academic, 1997, pp. 311–312.

[12] K. K. Kanazawa and J. G. Gordon, "Frequency of a quartz microbalance in contact with a liquid," *Anal. Chem.*, vol. 57, pp. 1770–1771, 1985.

[13] S. J. Martin, V. E. Granstaff, and G. C. Frye, "Characterization of a quartz crystal microbalance with simultaneous mass and liquid loading," *Anal. Chem.*, vol. 63, pp. 2272–2281, 1991.

[14] K. K. Kanazawa, "Steady state and transient QCM solutions at the metal/solution interface," *J. Electroanal. Chem.*, vol. 524–525, pp. 103–109, 2002.

[15] W. P. Mason, "Viscosity and shear elasticity measurements of liquids by means of shear vibrating crystals," *J. Colloid. Sci.*, vol. 3, pp. 147–162, 1948.

[16] B. A. Auld, *Acoustic Fields and Waves in Solids*, 2nd ed. Malabar, FL: Krieger, vol. 2, pp. 155–162.

[17] R. L. Steinfield, T. M. Fieser, R. A. Lerner, and I. A. Wilson, "Crystal structure of an antibody to a peptide and its complex with peptide antigen at 2.8 A," *Science*, vol. 248, pp. 712–719, 1990.

[18] J. M. Rini, U. Schulze-Gahmen, and I. A. Wilson, "Structural evidence for induced fit as a mechanism for antibody-antigen recognition," *Science*, vol. 255, pp. 959–965, 1992.

[19] E. A. Stura, G. G. Fieser, and I. A. Wilson, "Crystallization of antibodies and antibody–antigen complexes," *Immunomethods*, vol. 3, pp. 164–179, 1993.

[20] R. L. Stanfield, M. Takimoto-Kamimura, J. M. Rini, A. T. Profy, and I. A. Wilson, "Major antigen-induced domain rearrangements in an antibody," *Structure*, vol. 1, pp. 83–93, 1993.
[21] I. A. Wilson and R. L. Stanfield, "Antibody–antigen interactions: new structures and new conformational changes," *Current Opin. Struct. Biol.*, vol. 4, pp. 857–867, 1994.
[22] A. G. Amit, A. Mariuzza, S. E. V. Phillips, and R. J. Polijak, "Three-dimensional structure of an antigen–antibody complex at 2.8A resolution," *Science*, vol. 233, pp. 747–758, 1986.

Desmond D. Stubbs was born in Nassau, The Bahamas, in 1972. He received the B.S. degree in chemistry from Morris Brown College, Atlanta, GA, in 1997 and the M.S. degree in biochemistry from the Georgia Institute of Technology, Atlanta. He is working toward the Ph.D. degree in the School of Chemistry and Biochemistry, Georgia Institute of Technology. His doctoral thesis involves engineering proteins for biosensor applications.

From 1999 to 2001, he was a Demonstrations Teacher in the School of Chemistry, Georgia Institute of Technology.

William D. Hunt received the B.S. degree in electrical engineering from the University of Alabama, Tuscaloosa, in 1976, the M.S. degree in electrical engineering from the Massachusetts Institute of Technology, Cambridge, in 1980, and the Ph.D. degree in electrical engineering from the University of Illinois, Urbana-Champaign in 1987.

From 1976 to 1978, he was an Engineer with Harris Corporation. From 1980 to 1984, he was a Staff Engineer at Bolt Beranek and Newman Corporation, Arlington, VA. In 1987, he joined the electrical engineering faculty at Georgia Institute of Technology, Atlanta. His area of expertise is in the area of microelectronic acoustic devices for wireless applications as well as chemical and biological sensors based on this technology. He has published over 70 papers in refereed journals and conference proceedings. He holds four U.S. patents and five provisional patents.

Special recognitions that Dr. Hunt has received include the NSF Presidential Young Investigator Award in 1989, the DuPont Young Faculty Award in 1988, and the University of Alabama Distinguished Engineering Fellowship in 1994. He was a Rhodes Scholar Finalist in 1975.

Sang-Hun Lee was born in Seoul, Korea, in 1970. He received the B.Eng. degree in electronics engineering from Korea University, Seoul, in 1998 and the M.S. degree in electrical and computer engineering from the Georgia Institute of Technology, Atlanta, in 2000. He is currently working toward the Ph.D. degree in electrical engineering at the Georgia Institute of Technology as a Graduate Research Assistant.

His main research interest is in the design and fabrication of various acoustic wave devices for high-sensitivity chemical and biosensors.